JOURNAL OF MORPHOLOGY 265:87–101 (2005)

Limb Chondrogenesis of the Seepage Salamander, *Desmognathus aeneus* (Amphibia: Plethodontidae)

R. Adam Franssen,[1] Sharyn Marks,[2] David Wake,[3] and Neil Shubin[1]*

[1]*University of Chicago, Department of Organismal Biology and Anatomy, Chicago, Illinois 60637*
[2]*Humboldt State University, Department of Biological Sciences, Arcata, California 95521*
[3]*University of California, Museum of Vertebrate Zoology, Department of Integrative Biology, Berkeley, California 94720*

ABSTRACT Salamanders are infrequently mentioned in analyses of tetrapod limb formation, as their development varies considerably from that of amniotes. However, urodeles provide an opportunity to study how limb ontogeny varies with major differences in life history. Here we assess limb development in *Desmognathus aeneus*, a direct-developing salamander, and compare it to patterns seen in salamanders with larval stages (e.g., *Ambystoma mexicanum*). Both modes of development result in a limb that is morphologically indistinct from an amniote limb. Developmental series of *A. mexicanum* and *D. aeneus* were investigated using Type II collagen immunochemistry, Alcian Blue staining, and whole-mount TUNEL staining. In *A. mexicanum*, as each digit bud extends from the limb palette Type II collagen and proteoglycan secretion occur almost simultaneously with mesenchyme condensation. Conversely, collagen and proteoglycan secretion in digits of *D. aeneus* occur only after the formation of an amniote-like paddle. Within each species, Type II collagen expression patterns resemble those of proteoglycans. In both, distal structures form before more proximal structures. This observation is contrary to the proximodistal developmental pattern of other tetrapods and may be unique to urodeles. In support of previous findings, no cell death was observed during limb development in *A. mexicanum*. However, apoptotic cells that may play a role in digit ontogeny occur in the limbs of *D. aeneus*, thereby suggesting that programmed cell death has evolved as a developmental mechanism at least twice in tetrapod limb evolution. J. Morphol. 265:87–101, 2005.

KEY WORDS: chondrogenesis; limb development; salamander; apoptosis

The vertebrate limb has been described as "a powerful model system for studying the cellular and molecular interactions that determine morphological pattern during embryonic development" (Cohn and Bright, 1999:3). Indeed, the limb has been used for centuries as a model to address 1) the mechanisms of skeletal patterning (e.g., Schmalhausen, 1907, 1910; Holmgren, 1933; Shubin and Alberch, 1986), and 2) the evolutionary variability of developmental systems (e.g., Krause et al., 2004; Blanco and Alberch, 1992). Urodele amphibians provide a surprising source of variation of limb development. The statement by Cohn and Bright (1999) primarily referred to two amniote model systems (*Gallus*, chicken; *Mus*, mouse), on which most research has focused. However, the differences between urodeles and amniotes are so great that it has been proposed that the vertebrate limb may have evolved twice (Holmgren, 1933; Jarvik, 1965). Further, the differences between urodeles and anurans are significant enough to have suggested polyphyly within amphibians (Holmgren, 1933; Nieuwkoop and Sutasurya, 1976; Jarvik, 1965; reviewed by Hanken, 1986). Researchers have studied salamander morphology (e.g., Schmalhausen, 1915; Holmgren, 1933, 1939, 1942; Hinchliffe and Griffiths, 1986), described the patterns of amphibian limb development with reference to other tetrapods (Shubin and Alberch, 1986), and studied molecular pathways associated with amphibian limb and digit formation (e.g., Blanco et al., 1998; Cadinouche et al., 1999).

Salamanders and amniotes develop morphologically similar adult limbs despite differences in the molecular mechanisms driving limb outgrowth, the way in which digits form, and the sequence and timing of digit formation. For example, an apical ectodermal ridge (AER) regulates development of the proximal–distal axis during limb development in the chick (Saunders, 1948; Rubin and Saunders, 1972; Saunders et al., 1976; Riddle et al., 1993). The cells of the AER produce fibroblast growth factors (FGFs) that promote limb outgrowth (Niswander and Martin, 1992; Niswander et al., 1993; Savage et al., 1993; Fallon et al., 1994; Crossley and Martin, 1995). Additionally, the AER plays roles in feedback mechanisms with sonic hedgehog (SHH; e.g., Echelard et al., 1993; Krauss et al., 1993; Riddle et al.,

Contract grant sponsor: Division of Biological Sciences, University of Chicago.

*Correspondence to: Neil Shubin, University of Chicago, Department of Organismal Biology and Anatomy, 1027 E. 57th Street, Chicago, IL 60637. E-mail: nshubin@uchicago.edu

Published online 3 May 2005 in
Wiley InterScience (www.interscience.wiley.com)
DOI: 10.1002/jmor.10339

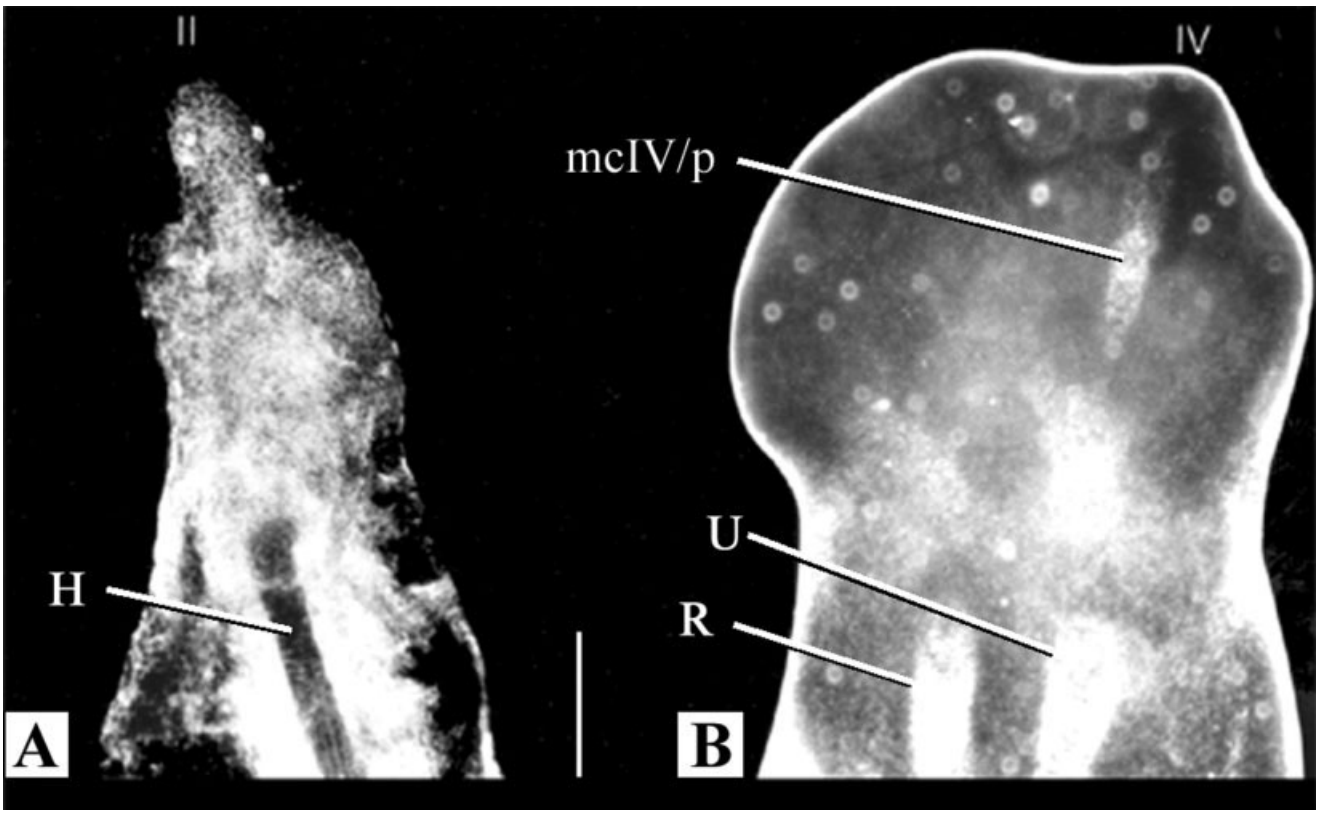

Fig. 1. Left forelimbs shown using darkfield microscopy. **A:** *Ambystoma mexicanum.* **B:** *Xenopus laevis.* II, Digit II; IV, Digit IV; H, humerus; mc, metacarpal; p, phalanx; R, radius; U, ulna. Scale bar = 0.125 mm.

1993; Roelink et al., 1994; Zeller et al., 1999; Panman and Zeller, 2003; Mic et al., 2004) and bone morphogenetic proteins (BMPs; Kingsley et al., 1992; Storm et al., 1994) to help regulate the dorsal–ventral and anterior–posterior axes (Johnson et al., 1994; Tickle and Eichele, 1994; Martin, 1998). Although FGFs have been identified in developing and regenerating salamander limbs (Han et al., 1997; Christensen et al., 2002), no AER has been identified. However, an apical ectodermal cap, which functions during regeneration much like an amniotic AER during normal development, is present in regenerating salamander limbs (Onda and Tassava, 1991). Another significant difference between salamanders and other tetrapods is sequence of digit formation. Amniotes develop their digits in a digital arch (Schmalhausen, 1910), with Digit IV forming first, and Digit I last (IV-V-III-II-I; Shubin and Alberch, 1986). However, salamanders develop their digital arch starting with Digit II and finishing with Digit V (II-I-III-IV-V; Shubin and Alberch, 1986; Wake and Shubin, 1998). This difference in digit sequence represents a shift in the formation of digits from posterior to anterior in amniotes, to anterior to posterior in salamanders. It is thought that amniote limbs form posteriorly first as a result of the action of SHH (Riddle et al., 1993). Sonic hedgehog is expressed in a gradient across the limb—strong expression in the posterior of the limb to weak expression in the anterior (Johnson and Tabin, 1995; Charitie et al., 2000; Lewis et al., 2001)—and helps regulate digit identity through the action of BMP2 (Drossopoulou et al., 2000). Sonic hedgehog is found in the posterior of the developing *Ambystoma* limb (Torok et al., 1999), but the role of BMPs is unknown. Furthermore, the reasons for the shift in digit order are unknown.

The morphology of digit formation is distinctively different in amniotes and urodeles. In amniotes, the limb bud extends distally and flattens horizontally into what appears to be a paddle (reviewed by Hanken, 1986; Shubin and Alberch, 1986). Digit condensation is then regulated by BMPs and FGFs (Dahn and Fallon, 2000; Sanz-Ezquerro and Tickle, 2003), and finally, BMP-mediated cell death removes the interdigital space, leaving independent digits (Fallon and Saunders, 1966; Dahn and Fallon, 2000). However, none of this occurs in larval salamanders, which lack a paddle stage. Rather, they develop digits as individual buds; each digit bud extends distally from the limb bud independently (Fig. 1; Holmgren, 1933; Shubin and Alberch, 1986), with little interdigital space in which BMPs and FGFs might act. Thus, the roles that apoptosis, BMPs, and

FGFs play in salamander limb development remain largely unknown. In addition, salamanders can regenerate limbs, have comparatively fewer cells, larger cells, larger genome sizes, and slower rates of development relative to amniotes (e.g., Martin and Gordon, 1995; Vignali and Nardi, 1996).

Urodele limb development not only differs from that of amniotes, it also varies among salamanders with different life-history strategies. There are three major life-history modes and each is associated with gross differences in the timing of development and morphologic specializations (Lombard and Wake, 1977; Wake and Larson, 1987). Pond dwellers (e.g., *Ambystoma mexicanum*) lay their eggs in lentic waters. Eggs are small and have relatively little yolk, so these larvae hatch quickly (about 22 days) and begin to feed. Hatchlings possess a well-developed head and their forelimbs are composed of Digits I, II, and III. As larvae grow, Digit IV of the forelimb develops, weeks before the appearance of the hindlimbs. Complete development of axolotl limbs takes at least 30 days at 22°C (Nye et al., 2003). Thus, the limbs, especially the forelimbs, constantly interact with the environment, which may affect their development. Stream-dwelling salamanders (e.g., *Desmognathus quadramaculatus*) have more yolk than pond dwellers, and hatch with a well-developed head and complete hind- and forelimbs. However, unlike direct-developers, they hatch as aquatic larvae and may require months or even years (2–4 years for *D. quadramaculatus*) before metamorphosing into morphologically distinct juveniles (Marks, 1995). Direct-developers (e.g., *D. aeneus*) develop into terrestrial juveniles without an intervening larval stage (Duellman and Trueb, 1986; Marks, 1995; Wake and Hanken, 1996). Eggs are laid terrestrially and contain a large amount of yolk that provides the embryo with a continuous source of food (Wake, 1982; Roth and Wake, 1985, 1989; Marks, 1995). One result of developing within the egg is a dramatic shift in the timing of events. Head development still occurs first, as is the case with pond dwellers, but it is followed much more closely by limb development. Additionally, the limbs develop much more synchronously than they do among pond dwellers; days separate the appearance of the hind- and forelimbs, rather than weeks. *Desmognathus aeneus* hatch after 68–75 days at 24°C, at which time they are (tiny) metamorphosed juveniles (Marks and Collazo, 1998). Additionally, all of the digits form nearly simultaneously in direct-developers (Marks and Collazo, 1998), rather than extending from the limb bud individually, as in the case of pond dwellers.

If we understand the differences in patterns of cartilaginous condensation, bone formation, and cell proliferation during limb development among urodeles—as well as between urodeles and amniotes—we can evaluate the generality of the described mechanisms of vertebrate limb development. We used cleared and stained whole mounts, immunohistochemistry, and antibody staining techniques to investigate the morphology of limb development and compare our results with those from amniote studies.

MATERIALS AND METHODS

Samples

Desmognathus aeneus eggs were collected from 22–26 May 2003 and 20 May–7 June 2004 from the Nantahala National Forest in the vicinity of Standing Indian Campground, Macon County, North Carolina. Animals were raised in the laboratory at 24°C as individual clutches on damp paper towels and sampled at all limb development stages based on Marks and Collazo (1998). *Ambystoma mexicanum* were ordered as wild-type embryos, juveniles, or larvae from the Indiana University Axolotl Colony (Bloomington, IN). Animals were raised at 22°C in Holtfreter's solution, as recommended. The staging tables of Harrison (1969) and Nye et al. (2003) were used to determine developmental stage. Embryos and larvae of both species were fixed using 4% paraformaldehyde (PFA), dehydrated through a methanol series, and stored at –20°C.

Alcian Blue

To stain for the demonstration of the proteoglycan component of cartilage using Alcian Blue, the protocol of Hanken and Wassersug (1981) was modified slightly. Samples were rehydrated from methanol and moved through a graded series to 70% ethanol. Because the salamanders were young, it was not necessary to skin and eviscerate them. The specimens were placed whole into a solution of 20 mg Alcian Blue, 70 ml 100% ethanol, and 30 ml glacial acetic acid for 6 h, after which they were transferred to ethanol/acetic acid overnight, and finally transferred to 100% ethanol. Specimens then were run through a graded series of ethanol/glycerol and stored in 100% glycerol.

Type II Collagen

To demonstrate the presence of Type II collagen, samples were rehydrated from methanol and rinsed three times in phosphate-buffered saline (PBS) with Tween-20 (PBT). Then they were bathed in 2.5% trypsin for 5 min (*Desmognathus aeneus*) or 15 min (*Ambystoma mexicanum*; because the *A. mexicanum* are larger, they require more time to digest). After three 5-min rinses in water, the samples were transferred to –20°C acetone for 10 min to increase penetrance. Specimens were rinsed in water for 10 min and then in PBT 3 times for 5 min before blocking for 1 h in a solution of PBS, DMSO, bovine serum, Tween-20, and water. Then they were incubated in an antibody against Type II collagen (II-II6B3; acquired from Hybridoma Bank, University of Iowa) diluted 1:100 in blocking solution overnight. After eight 15-min rinses in PBT plus 1% DMSO, specimens were placed in biotinylated secondary antibody in 1:500 blocking solution overnight. Samples were then washed eight times in PBT and incubated for 45 min in a biotinylated avidin complex. Then they underwent five 15-min rinses in PBT and three 10-min rinses in PBS and were bathed in a diaminobenzidine plus nickel chloride solution (Vectastain ABC Elite Kit, Vector Laboratories, Burlingame, CA). The reaction was stopped by washing with PBS followed by 50% ethanol. Specimens were then run through a graded series of ethanol/glycerol and stored in 100% glycerol.

Cell Death

The whole-mount TUNEL staining protocol was modified from the work of Blaschke et al. (1996). Animals were first anesthetized with a nonlethal dose of MS222 (Tricaine methanesulfonate) before sample limbs were amputated, fixed with PFA, and

stored in 100% methanol. Specimens were rehydrated to PBT and washed twice for 15 min in PBS before being washed twice for 30 min in terminal-deoxy-nucleotidyltransferase (TdT) buffer and then incubated overnight at room temperature in 150 U/ml TdT (Gibco, Grand Island, NY) and 0.5 mM dioxygenin – dUTP (Boehringer Mannheim, Germany). On the second day, specimens were washed twice for 30 min in PBT/EDTA followed by three 30-min washes in TBST. The samples then were presadsorbed in 10% fetal bovine serum (FBS)/TBST for 3 h and incubated overnight in 1% FBS/TBST plus 2μl anti-dig FAB fragments at 4°C. After three 20-min changes in 1% FBS/TBST, specimens were washed several times over a 2-day period in TBST. Samples then were washed three times for 20 min each in NTMT before being incubated in NTMT with bromo-4-chloro-3-indolyl-phosphate/nitro blue tetrazolium (BCIP/NBT; Sigmafast tablet, Sigma, St. Louis, MO, B-5655). This reaction turned apoptotic cells purple and was stopped with EDTA/PBT. Specimens then were transferred through a graded series to 100% glycerol and stored at 4°C.

Photography

Specimens were examined in glycerol at low resolution under a Heerbrugg M3C dissection scope and at high resolution using a Leitz Laborlux S light microscope. Photographs of the animals were taken using a Nikon Dlx digital camera, Nikon Capture Editor, and edited using PhotoShop 7.0 (Adobe Systems, San Jose, CA).

RESULTS

Chondrogenesis in *Desmognathus aeneus*

The *Desmognathus aeneus* stages described by Marks and Collazo (1998) are based on gross morphology and not on the internal aspects of limb patterning. Thus, numerous events of limb chondrogenesis may be lumped within a single developmental stage. Therefore, the stages in the following descriptions of proteoglycan and Type II collagen may vary slightly from the stages of Marks and Collazo (1998). Each stage of limb development lasts ~3 days at 24°C. Some of the earlier stages (e.g., 26 and 27) may last only 2 days, whereas the longest stages (30, 31) may last 5 days. The hind- and forelimbs of *D. aeneus* develop similarly; unless otherwise noted, the following descriptions are of forelimb development.

Stages 26 and 27 (Fig. 2). The limb of Stage 26 *Desmognathus aeneus* is long and narrow, with a rounded distal tip (Fig. 2A). In some specimens the pectoral girdle will take up Alcian stain (not shown). At this time, the humerus is represented only by a diffuse focus of Type II collagen stain, located in the proximal part of the limb bud (Fig. 2C).

By Stage 27, each of the four digits of the forelimb is distinct. The distal tip of the limb bud has small indentations between Digits I and II, II and III, and III and IV. However, no cartilaginous condensation of the digital elements has taken place (Fig. 2B). In addition, the limb is lengthened and long bones have differentiated to form the joint between the stylo- and zeugopodial elements. Condensation of cartilage of the entire humerus (H) and the proximal end of the radius (R) is visible with both staining techniques (Fig. 2B,D). Additionally, the ulna (U; slightly shorter than the radius) is visible with Type II collagen (Fig. 2D). Neither the radius nor ulna is completely condensed because the distal tips do not seem to have formed. The presence of stain in the humerus (Fig. 2C) and ulna (Fig. 2D) indicates that the Type II collagen component of cartilage forms slightly earlier in some stages than the proteoglycan component in these animals.

Stages 28 and 29 (Fig. 3). As the limb grows, condensations of the radius (R) and ulna (U) stain for proteoglycans (Fig. 3A) and Type II collagen (Fig. 3C). Neither has completed growth, however, because the distal caps have not differentiated. Metacarpal II (mcII) is quite distinct in the individual stained for Type II collagen; there is also a faint signal from the Alcian Blue stain in the same location. This is significant because in both cases this staining indicates that condensation of Metacarpal II occurs before condensation of either the meso- or metapodium, in contrast to the development in tetrapods that normally proceeds in a proximal-to-distal direction (reviewed by Hanken, 1986; Shubin and Alberch, 1986; Nye et al., 2003).

By Stage 29 the radius has stopped growing distally and has condensed into an autonomous unit (Fig. 3B,D). This coincides with the earliest formation of the radiale (r), intermedium (i), and ulnare (u). Each stains faintly with Alcian Blue. More distally, Metacarpal III begins to form (Fig. 3B), and there seems to be faint staining of Metacarpal I (Fig. 3B). Thus, the sequence of digit condensation proceeds as Digit II, Digit III, and then (based on the faint staining of Metacarpal I) Digit I. Proximal phalanges appear to form from the same condensation as the metacarpals; this can be seen quite clearly in Metacarpal III in both the Alcian Blue (Fig. 3B) and Type II collagen-labeled specimens (Fig. 3D).

At these stages, neither proteoglycans nor Type II collagen components of cartilage consistently appear before the other. For example, although Metacarpal II stains more darkly with Type II collagen than with Alcian Blue, it is present in both specimens (Fig. 3A,C). Additionally, the phalanx of Digit II and Metacarpal III are more darkly stained in the Type II embryos than in the Alcian Blue specimen (Fig. 3B,D); however, the radiale, ulnare, and intermedium stain only with Alcian Blue (Fig. 3B).

Stages 30–32 (Fig. 4). In Stage 30 embryos, Metacarpal I is stained with Alcian Blue before Element Y appears proximal to it (Fig. 4A). Element Y has Type II collagen staining and it is clear that Element Y and Metacarpal I form from different centers of condensation (Fig. 4D). Metacarpal I appears as a long condensation that segments distally to form the phalanx of Digit I. Element Y seems to form in the same condensation as the radiale (Fig. 4D), before clearly separating by Stage 31 (Fig. 4B), which is consistent with what has been observed in *Ambystoma mexicanum* (Shubin and Alberch, 1986). Indeed, at these stages there is evidence of a digital

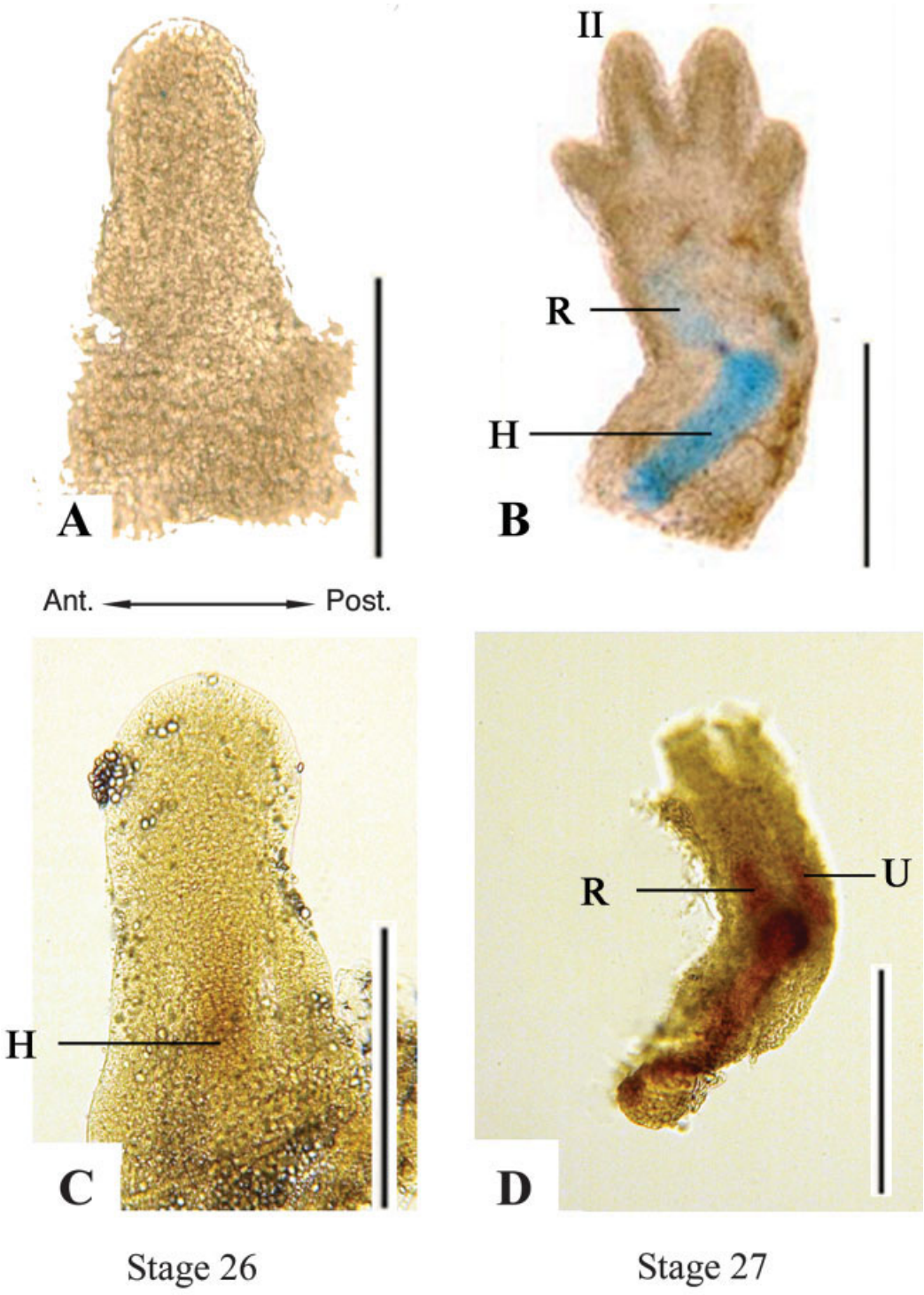

Fig. 2. *Desmognathus aeneus*. Dorsal view of left forelimbs at Stages 26 and 27. **A,B:** Stained with Alcian Blue. **C,D:** Stained using Type II collagen immunohistochemistry. II, Digit II; H, humerus; R, radius; U, ulna. Scale bar = 0.5 mm.

arch similar to that described by Shubin and Alberch (1986; Fig. 4A). The basale commune segments to form Distal Carpal 3, which then extends posteriorly toward the presumptive Distal Carpal 4 (Fig. 4A,B). Additionally, the ulnare condensation seems to segment distally and become Distal Carpal 4 (the two elements are still connected at Stage 30; Fig. 4A,D). Distal Carpal 4 then appears to segment distally to form Metacarpal IV (Fig. 4B,E). Similarly, the intermedium condenses and segments dis-

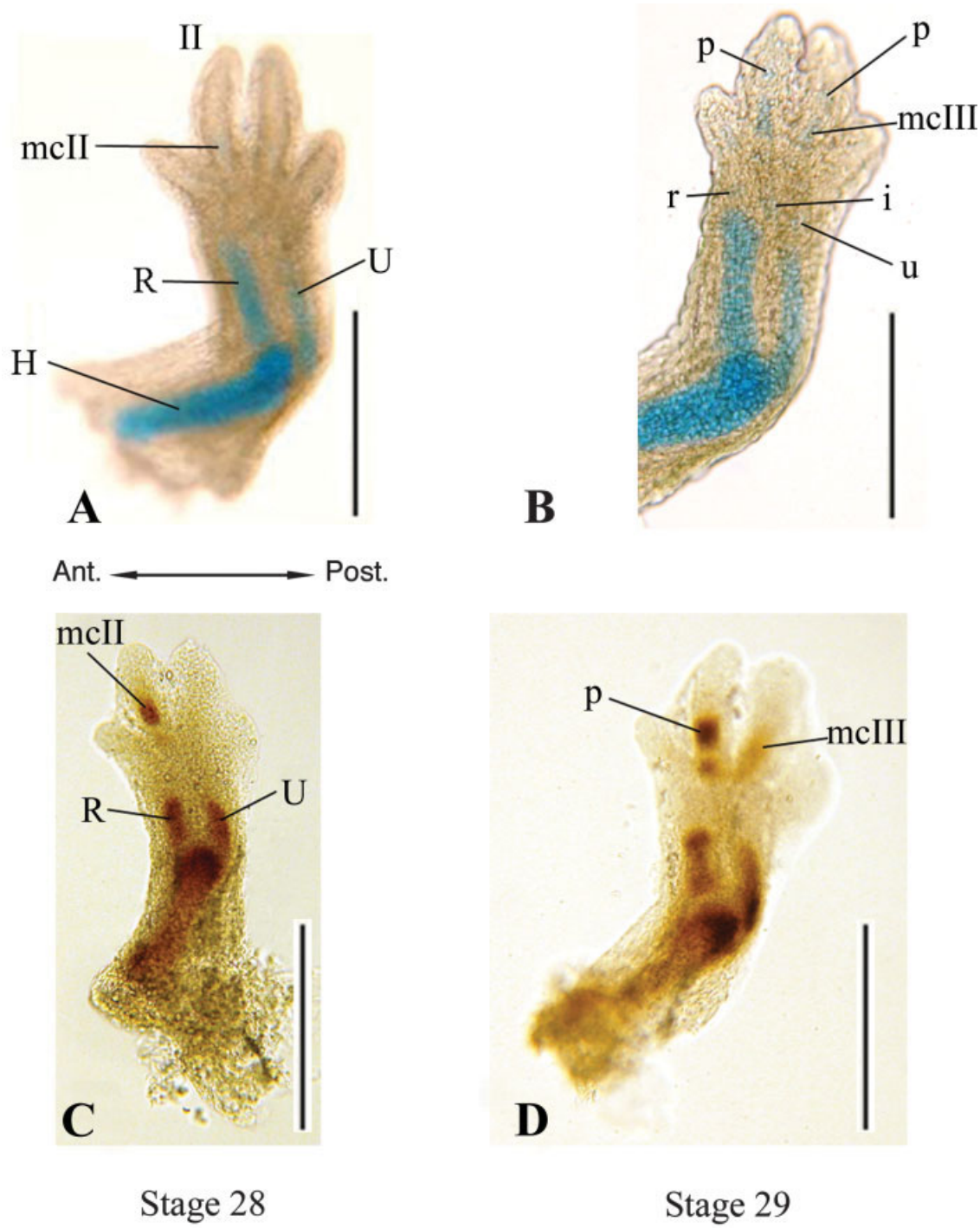

Fig. 3. *Desmognathus aeneus*. Dorsal view of left forelimbs at Stages 28 and 29. **A,B:** Stained with Alcian Blue. **C,D:** Stained using Type II immunohistochemistry. II, Digit II; H, humerus; i, intermedium; mc, metacarpal; p, phalanx; r, radiale; R, radius; U, ulna; u, ulnare. Scale bar = 0.5 mm.

tally to become the centrale (Fig. 4A,B). The centrale seems to then segment distally to produce the basale commune. This pattern of development is nearly identical to that which has been reported in the salamanders *Dicamptodon tenebrosus* (Wake and Shubin, 1998) and *Triturus marmoratus* (Blanco and Alberch, 1992).

By Stage 31, all of the meso- and metapodial elements are completely preformed in cartilage (Fig. 4B,E). The ulnare and Distal Carpal 4 seem to form when a single condensation splits into two distinct elements. The same is true for the radiale and Element Y. The centrale also is present at Stage 31 as a distinct element. By comparing Stages 30 and 31,

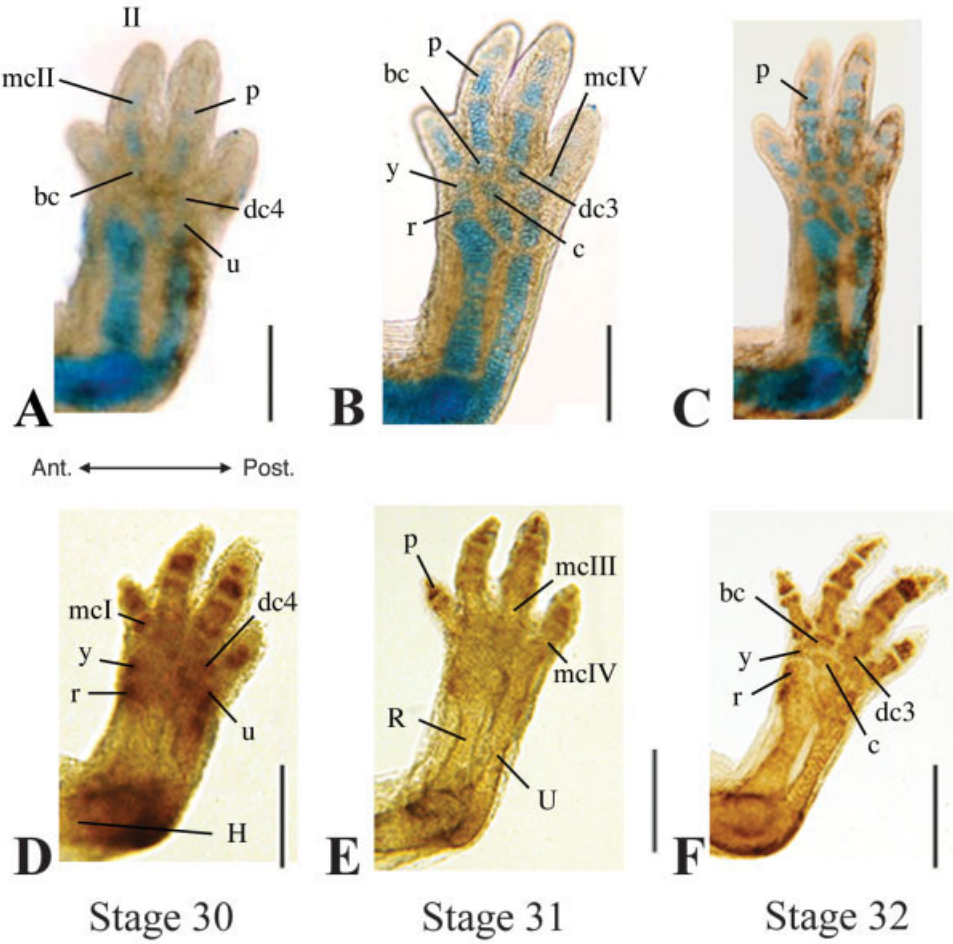

Fig. 4. *Desmognathus aeneus*. Dorsal view of left forelimbs at Stages 30–32. **A–C:** Stained with Alcian Blue. **D–F:** Stained using Type II immunohistochemistry. II, Digit II; bc, basale commune; c, centrale; dc, distal carpal; H, humerus; i, intermedium; mc, metacarpal; p, phalanx; r, radiale; R, radius; U, ulna; u, ulnare; y, Element Y. Scale bar = 0.25 mm.

we can conclude that as the intermedium condenses, a second center of condensation arises; the proximal center becomes the intermedium and the more distal center the centrale (Fig. 4A,B). This is consistent with the development of *Dicamptodon* (Wake and Shubin, 1998) and *Ambystoma* (Shubin and Alberch, 1986). Distal Carpal 3 stained with Alcian Blue as an individual element (Fig. 4B), but it is unclear how it arises. Most likely, it arose as part of a condensation forming the digital arch (Shubin and Alberch, 1986) including the ulnare and Distal Carpal 4. Additional condensation and staining of the phalanges continues at this stage. One phalanx of Digit I is distinct and another stains faintly with Alcian Blue at the distal tip of the digit (Fig. 4B). This second phalanx is more clearly defined in the Type II stained embryo (Fig. 4E). These phalanges seem to form as centers of condensation at the distal tips of the more proximal phalangeal and metacarpal condensations (Fig. 4A,B,D,E). Finally, cartilaginous condensations appear in Digit IV at Stage 31. Metacarpal IV may form from the same condensation as Distal Carpal 4. The first phalanx, however, appears to be condensing as an independent element (Fig. 4B,E). Based on the order of cartilaginous condensation, digit order in *Desmognathus aeneus* proceeds as II–III–I–IV.

By Stage 32, the final stage prior to hatching, nearly all of the elements of the manus are preformed in cartilage, including the terminal phalanx of Digits I and III (Fig. 4C,F). The only element not present at this stage is the terminal phalanx of Digit IV. This element would have formed after hatching and the resulting morphology would be consistent with previous observations (Shubin and Wake, 1996).

TUNEL Staining of *Desmognathus aeneus* (Fig. 5)

At Stage 26, whole-mount TUNEL staining does not reveal cell death in the forelimb; however, apoptosis does occur in the hindlimb. There are three strips of apoptotic cells at the distal tip of the hindlimb (Fig. 5D; arrows). The most anterior strip ap-

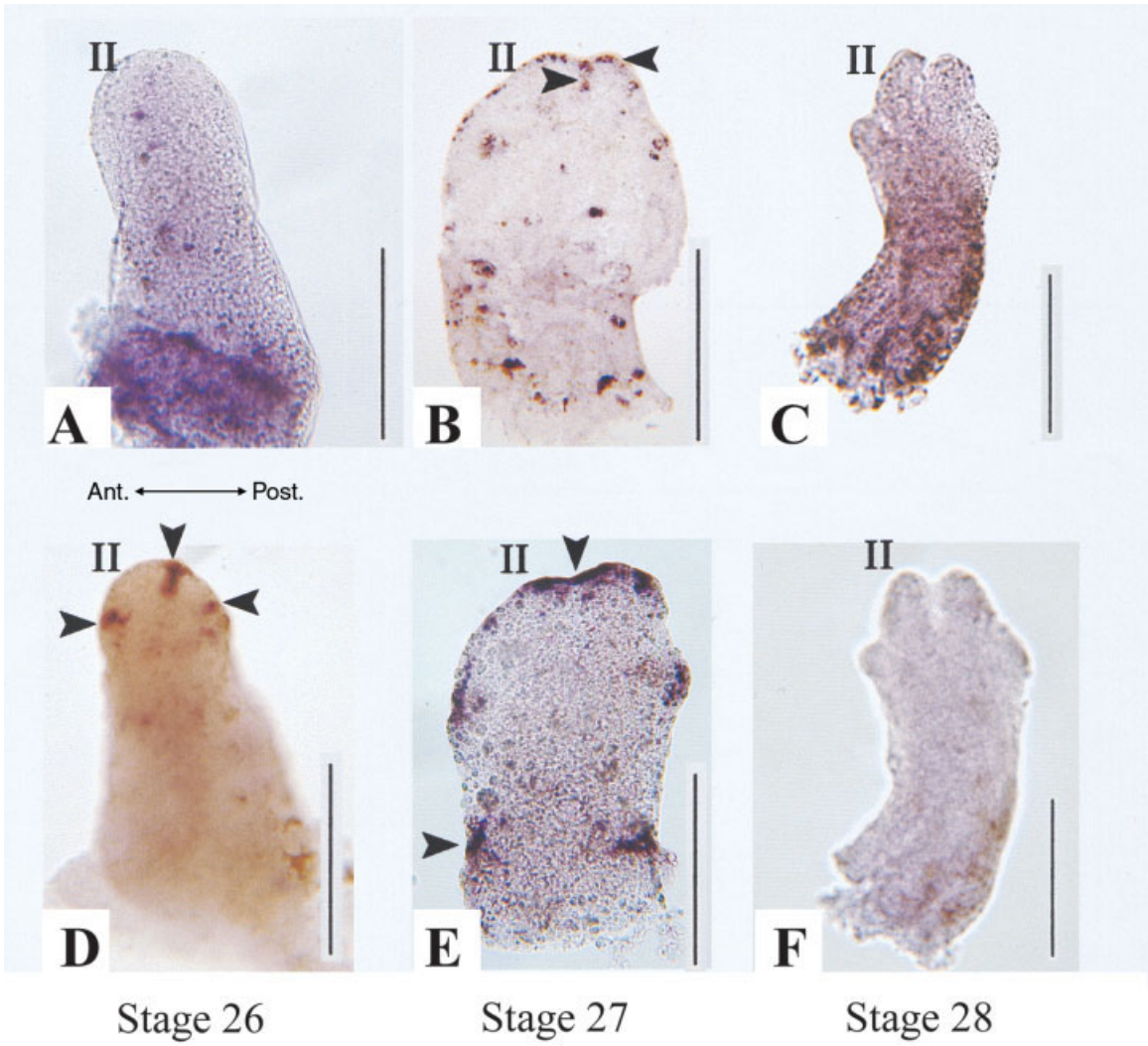

Fig. 5. *Desmognathus aeneus.* TUNEL stained to show apoptotic cells at Stages 26–28. **A–C:** Dorsal view of left forelimbs. **D–F:** Dorsal view of left hindlimbs. Arrows indicate areas of staining. II, Digit II. Scale bar = 0.5 mm.

pears to be located at what will be the indentation between Digits I and II, the middle strip appears to be located at what will be the indentation between Digits II and III, and the most posterior strip, which is the least defined, appears to be at the division between Digits III and IV.

Apoptosis occurs in both the hind- and forelimbs of Stage 27 samples. In the forelimb there is a ridge of cell death along the distal tip of the limb, including a strip of apoptotic cells in a small indentation that will likely become the division between Digits II and III (Fig. 5B; arrow). A similar staining pattern is seen in the hindlimb at this stage; the staining appears to be more intense at the distal tip, but a defined strip such as that seen in Stage 26 of the hindlimb or Stage 27 of the forelimb is absent (Fig. 5E). Additional cell death is present on both the anterior and posterior sides of the limb, proximal to the presumptive digits. These regions of staining appear to be located at what will be the elbow or knee joints.

At Stage 28 apoptotic zones are absent. Samples treated with the TUNEL technique at this stage, as well as later stages (not shown), do not stain, indicating that cell death may not occur past Stage 27. Significantly, the interdigital tissues have receded between Digits I and II, as well as Digits II and III. This supports the hypothesis that apoptosis at Stages 26 and 27 helped form these indentations.

Chondrogenesis in *Ambystoma mexicanum*

Limb development has been well studied using Alcian Blue (e.g., Muneoka and Bryant, 1982; Shubin and Alberch, 1986; Nye et al., 2003). Here, our goal is to directly compare the timing of proteoglycan condensation with that of Type II collagen.

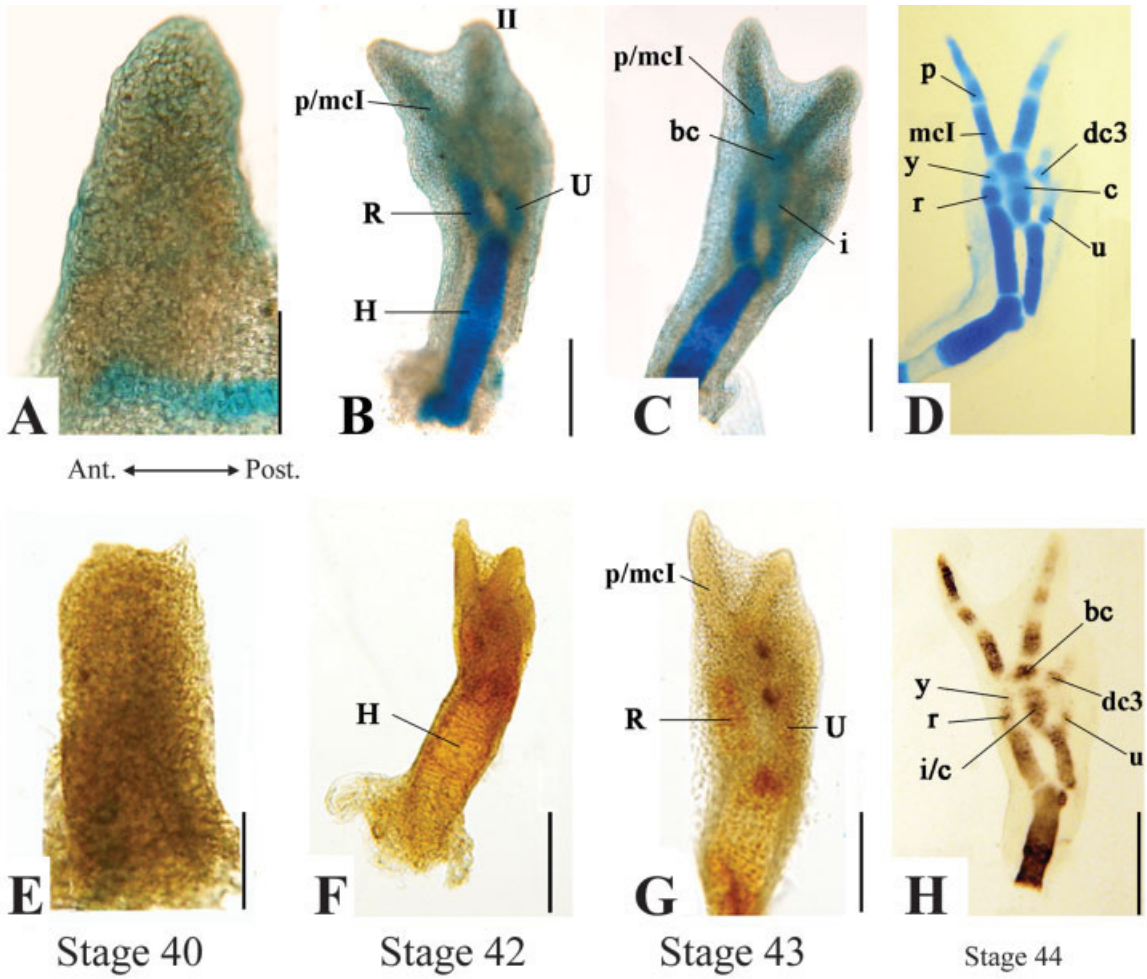

Fig. 6. *Ambystoma mexicanum*. Dorsal view of left forelimbs at Stages 40–44. **A–D:** Stained with Alcian Blue. **E–H:** Stained using Type II immunohistochemistry. II, Digit II; bc, basale commune; c, centrale; dc, distal carpal; H, humerus; i, intermedium; mc, metacarpal; p, phalanx; R, radius; r, radiale; U, ulna; u, ulnare; y, Element Y. Scale bar = 0.25 mm.

Stages 40–44 (Fig. 6). By Stage 40 the axolotl limb bud is long and narrow; it has a rounded distal tip and lacks formation of any digits (Fig. 6A,E). Although the pectoral girdle can be seen as a thin line of Alcian Blue stain (Fig. 6A), there does not seem to be any condensation of limb elements.

By Stage 42 the limb bud has extended and bends at the presumptive joint between the stylopod and zeugopod. The humerus is completely stained with Alcian Blue (Fig. 6B) and Type II collagen (less intense; Fig. 6F), indicating that the bone is preformed in cartilage and that proteoglycans are present throughout (Fig. 6B). Only several cells wide, the humerus has condensed completely and the joint between the zeugopod and stylopod has formed (Fig. 6B,F). Distal to the humerus, the proximal halves of the radius and ulna also show the presence of both proteoglycans (Fig. 6B) and Type II collagen (faintly; Fig. 6F). However, the distal half, which joins the autopod, is unstained at this stage, indicating that both elements continue to condense distally. In contrast to the developmental pattern of most tetrapods (in which digits IV and V form first), Digits II and I emerge as individual digit buds from the limb bud at this time. Interdigital tissues are present between the two digits, and although each digit is distinct at the most distal tip, the presence of any interdigital tissue is previously unreported for *Ambystoma mexicanum* (Fig. 6B,F). Digit I extends distal to the radius. Metacarpal I and the most proximal phalanx of Digit I have condensed as a single element and stain with Alcian Blue (Fig. 6B). Again, a single condensation can be seen in Digit I of the embryo stained for Type II collagen, but staining is faint (Fig. 6F). Although Digit II has also emerged as an individual bud, no phalanges have condensed at this time.

At Stage 43 (Fig. 6C,G) the radius and ulna continue to extend distally and are beginning to differentiate into individual elements. A single condensation that forms between the radius and ulna extends proximally from the presumptive intermedium to

the basale commune. Although consistent with previous descriptions of *Ambystoma* (Shubin and Alberch, 1986), this pattern differs significantly from that observed in *Desmognathus aeneus*, in which the basale commune appears to condense independently of the intermedium and centrale. In axolotls, the basale commune, although most distal, appears first and segments from the rest of the condensation before either the centrale or intermedium (Fig. 6C,D,H). Stage 43 limbs also show additional staining of the phalanges in Digits I and II. In both digits a single, continuous, cartilaginous condensation of the phalanges is present; this condensation splits into the individual phalangeal elements of each digit (Fig. 6D). Interdigital tissue can still be seen between Digits I and II at this time. Furthermore, it appears that Digits III and IV are starting to develop on the posterior side of the limb. These digits are still connected to the limb and Digit II via interdigital tissue.

By Stage 44 most zeugopodial and autopodial elements are defined. The ulna and radius have formed completely. In the mesopodium the ulnare, intermedium, radiale, Element Y, and basale commune have condensed and are stained with Type II collagen and Alcian Blue (Fig. 6D,H). The boundaries of the centrale remain faint, indicating that it is not yet completely separated from the intermedium (Fig. 6D). Type II staining still shows the two elements as a single condensation at this time (Fig. 6H). The metapodium consists only of Distal Carpal 3. Between the more distinct forms of the ulnare and Distal Carpal 3 there remains a faint condensation that eventually segments to form Distal Carpal 4 (Fig. 6D). Thus, there are two digital arches that form in the axolotl—one connecting the centrale, intermedium, and basale commune, and another connecting the ulnare, Distal Carpal 4, and Distal Carpal 3. These results are consistent with those of Shubin and Alberch (1986). Further, the metacarpals and two distal phalanges of Digits I and II, as well as Metacarpal III, have condensed and can be visualized with both the Alcian Blue and Type II collagen (Fig. 6D,H). Interdigital tissue is no longer present. In all of the embryos from Stages 40–42 the same elements are seen with both Alcian Blue and Type II collagen. However, the staining for Alcian Blue is much more intense. Possibly, Type II collagen does not fully incorporate into the cartilage until stage 44.

Stages 45 and 46 (Fig. 7). Stage 45 limbs are similar to those of Stage 44. The distal phalange of Digit II is completely condensed and Digit III continues to extend distally; Metacarpal III is condensing, but is not yet distinct from the phalanges. Embryos stained for Type II collagen have nearly identical developmental patterns to those stained for Alcian Blue. There appears to be only slight variation in the intensity of staining of certain elements. For example, the radiale, ulnare, and basale commune stain much more darkly with Alcian Blue at this stage (Fig. 7A), perhaps indicating slightly more incorporation of proteoglycans versus Type II collagen at this stage.

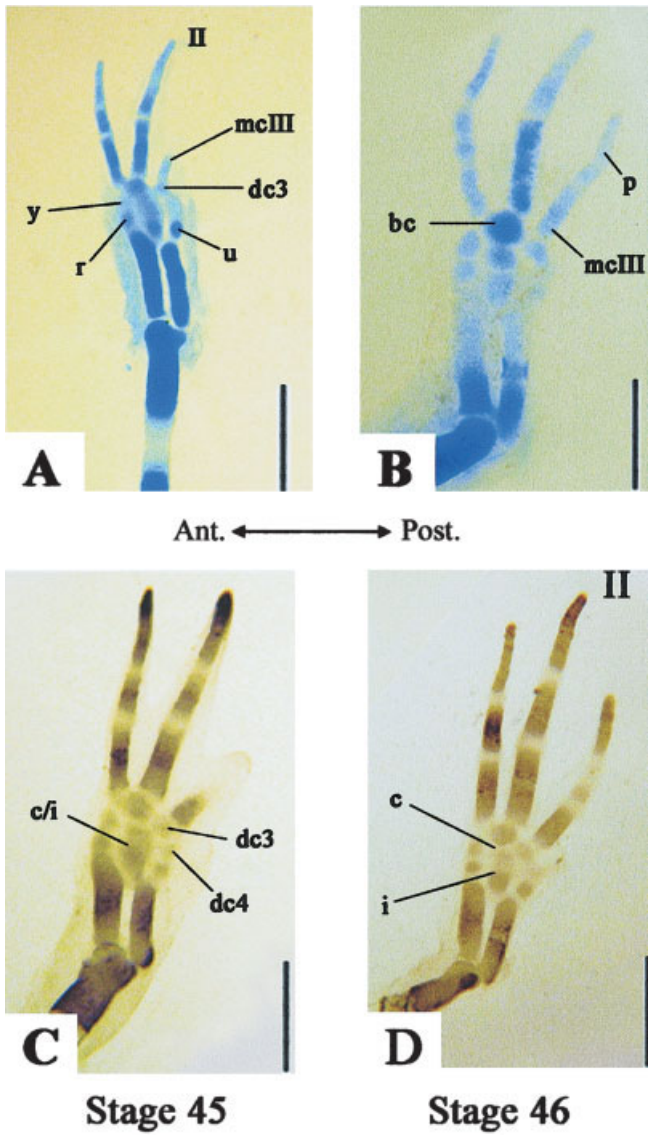

Fig. 7. *Ambystoma mexicanum*. Dorsal view of left forelimbs at Stages 45 and 46. **A,B:** Stained with Alcian Blue. **C,D:** Stained using Type II immunohistochemistry. II, Digit II; bc, basale commune; c, centrale; dc, distal carpal; i, intermedium; mc, metacarpal; p, phalanx; r, radiale; u, ulnare; y, Element Y. Scale bar = 0.25 mm.

Stage 46 individuals are distinguished by the separation of the centrale from the intermedium (Fig. 7B). Although they clearly form from the same original condensation, their individual condensation centers have grown enough to identify each as an independent element (Fig. 7D). Digit III continues to extend distally; by this stage, two phalanges are seen distal to Metacarpal III. The phalanges appear to be forming as one continuous

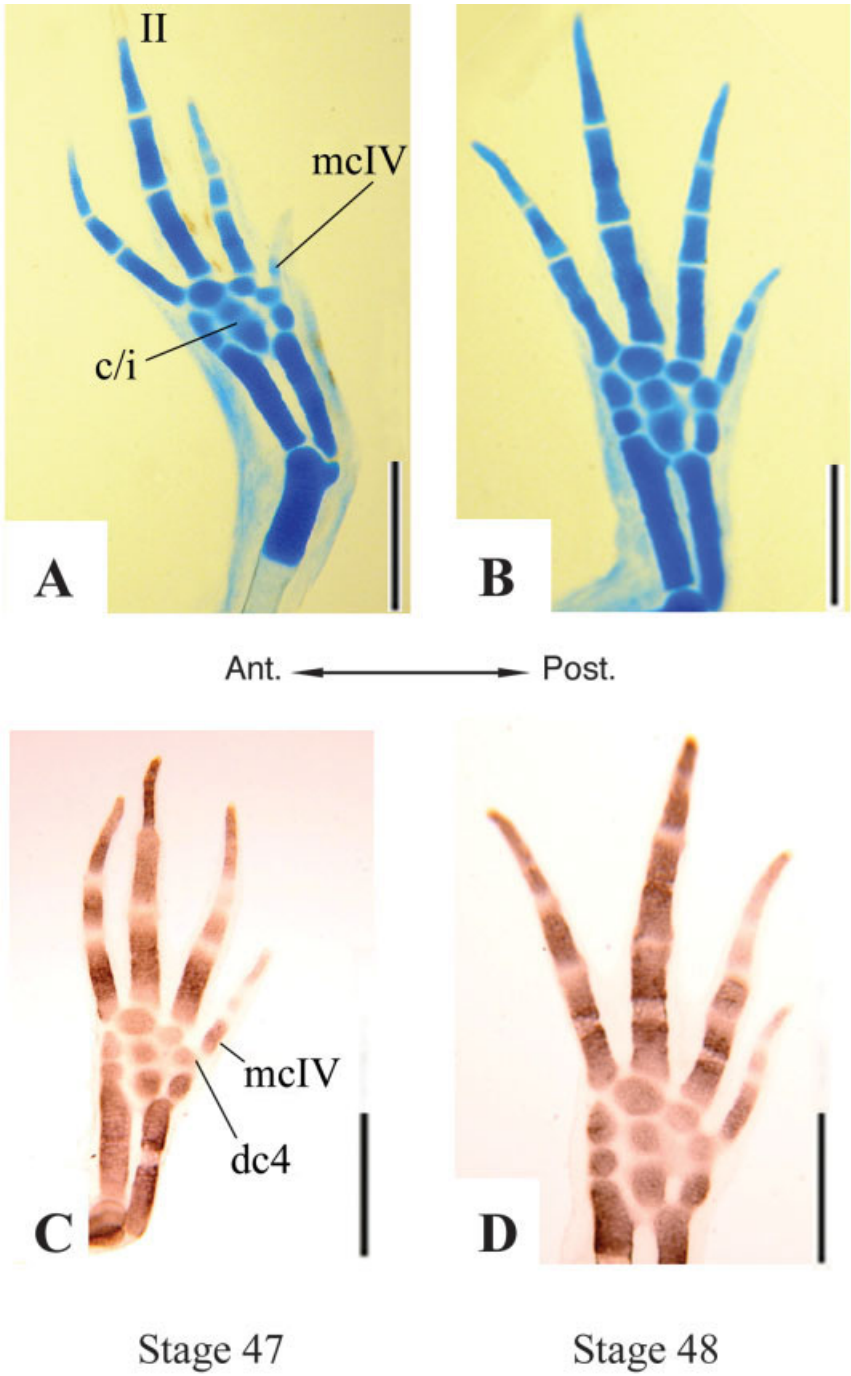

Fig. 8. *Ambystoma mexicanum*. Dorsal view of left forelimbs at Stages 47 and 48. **A,B:** Stained with Alcian Blue. **C,D:** Stained using Type II immunohistochemistry. II, Digit II; c, centrale; i, intermedium; mc, metacarpal; p, phalanx. Scale bar = 0.25 mm.

cartilaginous condensation and then breaking off from one another.

By Stages 45 and 46 the relative contributions of Type II collagen and proteoglycans to cartilage appear to be equal.

Stages 47 and 48 (Fig. 8). In Stage 47 embryos (Fig. 8A) Digit IV has begun to bud off from the limb bud. Interestingly, the intermedium and centrale remain fused in these specimens; Stage 46 embryos showed the intermedium and centrale as individual elements. That they are still fused at Stage 47 in these embryos indicates that the order of appearance of elements varies between individuals. Metacarpal IV has condensed completely, the first and third phalanges are distinct, and the second phalanx is stained faintly (Fig. 8C). This suggests that the phalanges are indeed

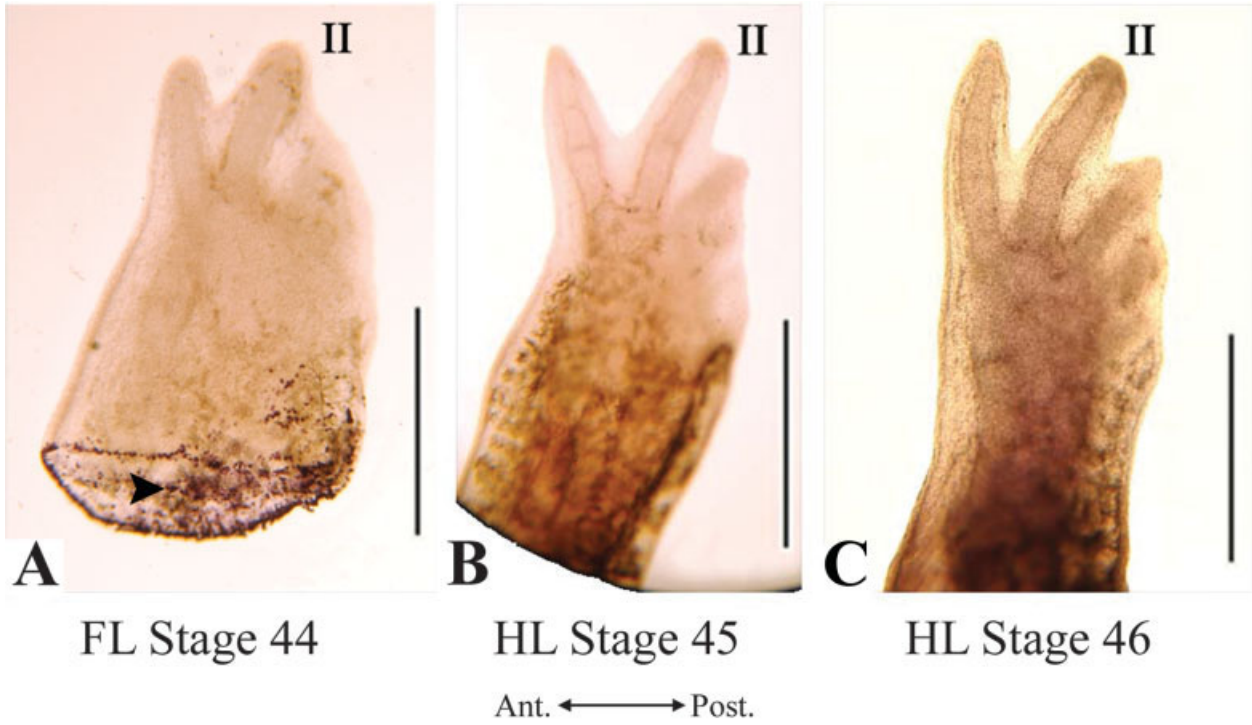

Fig. 9. *Ambystoma mexicanum.* TUNEL-stained to show apoptotic cells. **A:** Dorsal view of left forelimb at Stage 44. **B:** Dorsal view of left hindlimb at Stage 45. **C:** Dorsal view of left hindlimb at Stage 46. Arrows indicate areas of staining. II, Digit II. Scale bar = 0.5 mm.

forming as a single, continuous condensation, rather than as individual condensations.

By Stage 48 all of the elements of the manus are present. The stylopod and zeugopod are completely formed, as are all of the meso- and metapodial elements. Digits I and II have three phalanges, Digit III has all four phalanges, and Digit IV has three complete phalanges (Fig. 8B,D).

Although Type II collagen and Alcian Blue staining reveal a similar pattern of digit development, the Type II embryos more clearly reveal (with darker staining) distal elements forming before more proximal elements during these stages.

Cell Death in *Ambystoma mexicanum* (Fig. 9)

Cell death was not seen in the interdigital spaces of developing axolotl limbs in either the hind- (Fig. 9B,C) or forelimbs (Fig. 9A). Although there is no discernable staining at the distal tip of the limb, there is significant staining (Fig. 9A; purple dots, arrow) in the proximal part of the limb. The same is true for the distal ends of the hindlimbs (not shown). Thus, cells at the amputation point died and were appropriately labeled. This result is consistent with the results of previous studies (Vlaskalin et al., 2004).

DISCUSSION

Our results indicate that *Desmognathus aeneus* forms limbs in a novel way compared to *Ambystoma mexicanum*. Indeed, in some respects *D. aeneus* limb development is more similar to amniote limb development than to that of axolotls. The most significant distinction between the developing limb of *D. aeneus* and *A. mexicanum* is the outgrowth of the digits. In both species the limb bud extends from the body wall and continues to lengthen distally as the precartilage foci of the humerus, radius, and ulna begin to condense. The timing of digit appearance varies between the two species. In *A. mexicanum*, each digit extends from the limb bud as its own individual bud. Within each bud, the metapodials and phalanges condense and segment from one another. These internal processes of cartilage formation are coincident with the elongation of the digital bud. The first digit to bud at the distal tip of the limb is Digit II (Fig. 6B,F). The mesenchymal template of the digit extends from the limb, the cartilaginous condensation of the phalanges begins, and then the next digit begins to bud from the limb bud. Indeed, cartilaginous condensation of Digit III is complete before Digit IV even begins to bud. In *D. aeneus*, however, the limb bud extends from the body wall and begins to flatten at the distal tip, forming a paddle similar to what is seen during amniote limb development (Fig. 2A). External furrows appear between each

digital primordium before evidence of a cartilage formation of metapodials and phalanges. Only once the mesenchymal template for the digits has formed (Fig. 2B) does cartilaginous condensation of the digital elements take place (Fig. 3E,G). The differences between these taxa suggest that there is a disparity in the timing of the key events of digital formation: condensation, cartilage matrix secretion, and sculpting of the interdigital spaces between the digital primordial.

Study of these two urodele species has also revealed differences in the role of apoptosis in morphogenesis. Although researchers have not found cell death during normal development in *Ambystoma mexicanum* (Cameron and Fallon, 1977), the discovery of interdigital tissue between Digits I and II (in which cell death might play a role in digit ontogeny) required additional study. However, our results with axolotls support previous findings (Cameron and Fallon, 1977). Cell death was detected in *Desmognathus aeneus* at the presumptive interdigital spaces in both the forelimbs and hindlimbs. The programmed cell death at the distal tip helps form the mesenchymal template for *D. aeneus* digits, which precedes digital condensation. This contrasts with the situation in amniotes, in which a paddle-stage forms first at the distal tip of the limb bud, followed by the condensation of digital elements within the paddle, which are then distinguished from one another by apoptosis. Although the staining was not as pronounced in *D. aeneus*, as would be expected from amniotes, the results are still significant. Urodele cells are much larger than those of amniotes; thus, only a fraction of the number of cells in an amniote limb is present in the developing salamander limb. Additionally, because the stages in which we see cell death take ~5 or 6 days to complete, it is fortunate that we could observe dying cells. The presence of apoptotic cells suggests not only heterogeneity of morphological development between these two urodele species, but also a significant difference in the timing of gene expression. Exploration of BMP expression in *D. aeneus* and *A. mexicanum* is critical to understanding the mechanisms behind this variation.

The presence of cell death in *Desmognathus aeneus* also raises questions about the evolutionary history of apoptosis in tetrapods. Cell death has been reported in the limbs of birds (e.g., Dahn and Fallon, 2000), mammals (e.g., Zakeri and Ahuja, 1994), and reptiles (e.g., Fallon and Cameron, 1977; Goel and Mathur, 1978; Sorenson and Mesner, 2005), but not in amphibians (Cameron and Fallon, 1977). It is possible that cell death is absent in most urodeles, but evolved independently in *D. aeneus* and amniotes. Alternatively, most urodeles may indeed use programmed cell death during limb development and only a few species, such as *Ambystoma mexicanum* and *Notopthalmus viridescens* (Vlaskalin et al., 2004), have lost apoptosis as a developmental mechanism. More species of urodeles must be investigated to resolve this issue.

Desmognathus aeneus and *Ambystoma mexicanum* also differ with regard to the sequence of digit condensation. In *A. mexicanum*, Digit II begins to form first, followed by Digits I, III, and IV. However, in *D. aeneus*, Digit II forms first, followed by Digits III, I, and IV. Neither order is identical to that of amniotes. These differences in timing of cartilaginous condensation certainly indicate variation in the timing or location of gene expression. Exploration of genes such as SHH and Sox9 could greatly enhance our understanding of how digit condensation is triggered.

Our findings indicate that tetrapod limb development is extremely variable. Indeed, concepts that frame the basis for the tetrapod model of limb development, things that are often taken for granted—that limb development proceeds proximally to distally, that digits form posteriorly to anteriorly, that cell death occurs after digit formation and only in amniotes—are not even true for all groups of salamanders. What we have discovered in working with a direct-developing salamander is a source of variability in the tetrapod lineage that is likely a target of natural selection. Evolution of specialized life history modes in salamanders has involved novel disassociations among the sequence of cartilage condensation, digit elongation, and the utilization of interdigital spaces. Further study of the developmental programs of each life history mode will likely reveal a link between developmental biology, ecology, and evolution in this clade.

ACKNOWLEDGMENTS

Our research was made possible by permits from the United States Forest Service (permit #FS-2700-25) and the North Carolina Wildlife Resources Commission (permit #0370). K. Franssen, C. Lowry, and P. Warny assisted greatly with collection of *Desmognathus aeneus*. The Highlands Biological Station kindly provided the space and microscopes to inspect salamander clutches while in Highlands, NC.

LITERATURE CITED

Blanco MJ, Alberch P. 1992. Caenogenesis, developmental variability, and evolution in the carpus and tarsus of the marbled newt, *Triturus marmoratus*. Evolution 46:677–687.

Blanco MJ, Misof BY, Wagner GP. 1998. Heterochronic differences of Hoxa-11 expression in *Xenopus* fore- and hind limb development: evidence for lower limb identity of the anuran ankle bones. Dev Gene Evol 208:175–187.

Blaschke AJ, Staley K, Chun J. 1996. Widespread programmed cell death in proliferative and postmitotic regions of the fetal cerebral cortex. Development 122:1165–1174.

Cadinouche MZA, Liversage RA, Muller W, Tsilfidis C. 1999. Molecular cloning of the *Notophthalmus viridescens* radical fringe cDNA and characterization of its expression during forelimb development and adult forelimb regeneration. Dev Dyn 214:259–268.

Cameron JA, Fallon JF. 1977. The absence of cell death during development of free digits in amphibians. Dev Biol 55:331–338

Charitie J, McFadden DG, Olson EN. 2000. The bHOL transcription factor dHAND controls sonic hedgehog expression and establishment of the zone of polarizing activity during limb development. Development 127:2461–2470.

Christensen RN, Weinstein M, Tassava RA. 2002. Expression of fibroblast growth factors 4, 8, and 10 in limbs, flanks, and blastemas of Ambystoma. Dev Dyn 223:193–203.

Cohn MJ, Bright PE. 1999. Molecular control of vertebrate limb development, evolution and congenital malformations. Cell Tissue Res 296:3–17.

Crossley PH, Martin GR. 1995. The mouse Fgf8 gene encodes a family of polypeptides and is expressed in regions that direct outgrowth and patterning in the developing embryo. Development 121:439–451.

Dahn RD, Fallon JF. 2000. Interdigital regulation of digit identity and homeotic transformation by modulated BMP signaling. Science 21:289:438–441.

Drossopoulou G, Lewis KE, Sanz-Ezquerro JJ, Nikbakht N, McMahon AP, Hoffman C, Tickle C. 2000. A model for anterioposterior patterning of the vertebrate limb based on sequential long- and short-range Shh signaling and Bmp signaling. Development 127:1337–1348.

Duellman W, Trueb L. 1994. Biology of Amphians. New York: McGraw-Hill.

Echelard Y, Epstein DJ, St-Jacques B, Shen L, Mohler J, McMahon JA, McMahon AP. 1993. Sonic hedgehog, a member of a family of putative signaling molecules, is implicated in the regulation of CNS polarity. Cell 31:1417–1430.

Fallon JF, Cameron J. 1977. Interdigital cell death during limb development of the turtle and lizard with an interpretation of evolutionary significance. J Embryol Exp Morphol 40:285–289.

Fallon JF, Saunders JW. 1966. Reversibility of commitment to morphogenetic cell death in wing bud tissues of chick embryo. Am Zool 6:328.

Fallon JF, Lopez A, Ros MA, Savage MP, Olwin BB, Simandl BK. 1994. FGF-2: apical ectodermal ridge growth signal for chick limb development. Science 264:104–107.

Goel SC, Mathur JK. 1978. Cell death in reptilian limb morphogenesis. Indian J Exp Biol 16:653–655.

Han MJ, Chung HM, Nham SU, Kim WS. 1997. Partial cloning of FGF-8 cDNA in Mexican axolotl, *Ambystoma mexicanum*. Korean J Gen 19:169–176.

Hanken J. 1986. Developmental evidence for amphibian origins. Evol Biol 20:389–417.

Hanken J, Wassersug RJ. 1981. The visible skeleton. Funct Photog 16:22–26.

Harrison RG. 1969. Organization and development of the embryo. New Haven, CT: Yale University Press.

Hinchliffe JR, Griffiths PJ. 1986. Vital staining for cell death in chick limb buds: a histochemical technique in the analysis of control of limb development. Acta Histochem Suppl 32:159–164.

Holmgren N. 1933. On the origin of the tetrapod limb. Acta Zool 14:185–295.

Holmgren N. 1939. Contribution on the question of the origin of the tetrapod limb. Acta Zool 20:89–124.

Holmgren N. 1942. On the origin of the tetrapod limb—again. Acta Zool 30:485–508.

Jarvik E. 1965. On the origin of girdles and paired fins. Israel J Zool 14:141–172.

Johnson RL, Tabin C. 1995. The long and short of hedgehog signaling. Cell 81:313–316.

Johnson RL, Laufer E, Riddle RD, Tabin C. 1994. Ectopic expression of Sonic hedgehog alters dorsal-ventral patterning of somites. Cell 79:1165–1173.

Kingsley DM, Bland AE, Grubber JM, Marker PC, Russell LB, Copeland LG, Jenkins NA. 1992. The mouse *short ear* skeletal morphogenesis locus is associated with defects in a bone morphogenetic member of the TGF-b superfamily. Cell 71:399–410.

Krause A, Zacharias W, Camarata T, Linkhart B, Law E, Lischke A, Miljan E, Simon HG. 2004. Tbx5 and Tbx4 transcription factors interact with a new chicken PDZ-LIM protein in limb and heart development. Dev Biol 273:106–120.

Krauss S, Concordet JP, Ingham PW. 1993. A functionally conserved homolog of the Drosophila segment polarity gene hh is expressed in tissues with polarizing activity in zebrafish embryos. Cell 75:1431–1444.

Lewis PM, Dunn MP, McMahon JA, Logan M, Martin JF, St-Jacques B, McMahon AP. 2001. Cholesterol modification of sonic hedgehog is required for long-range signaling activity and effective modulation of signaling by Ptc1. Cell 105:599–612.

Lombard RE, Wake DB. 1977. Tongue evolution in lungless salamanders, Family Plethodontidae. II. Function and evolutionary diversity. J Morphol 153:39–80.

Marks SB. 1995. Development and evolution of the dusky salamanders (genus *Desmognathus*). Dissertation, University of California, Berkeley.

Marks SB, Collazo A. 1998. Direct development in *Desmognathus aeneus* (Caudata: Plethodontidae): a staging table. Copeia 3:637–648.

Martin GR. 1998. The roles of FGFs in the early development of vertebrate limbs. Genes Dev 12:1571–168.

Martin CC, Gordon R. 1995. Differentiation trees, a junk DNA molecular clock, and the evolution of neoteny in salamanders. J Evol Biol 8:339–354.

Mic FA, Sirbu IO, Duester G. 2004. Retinoic acid synthesis controlled by Raldh2 is required early for limb bud initiation and then later as a proximodistal signal during apical ectodermal ridge formation. J Biol Chem 279:26698–26706.

Muneoka K, Bryant SV. 1982. Evidence that patterning mechanisms in developing and regenerating limbs are the same. Nature 298:396–371.

Nieuwkoop PD, Sutasurya LA. 1976. Embryological evidence for a possible polyphyletic origin of recent amphibians. J Embryol Exp Morphol 35:159–167.

Niswander L, Martin GR. 1992. FGF-4 and BMP-2 have opposite effects on limb growth. Nature 361:68–71.

Niswander L, Tickle C, Vogel A, Booth I, Martin GR. 1993. FGF-4 replaces the apical ectodermal ridge and directs outgrowth and patterning of the limb. Cell 75:579–587.

Nye HL, Cameron JA, Chernoff EA, Stocum DL. 2003. Extending the table of stages of normal development of the axolotl: limb development. Dev Dyn 226:555–560.

Onda H, Tassava RA. 1991. Expression of the 9G1 antigen in the apical cap of axolotl regenerates requires nerves and mesenchyme. J Exp Zool 257:336–349.

Panman L, Zeller R. 2003. Patterning the limb before and after SHH signaling. J Anat 202:3–12.

Riddle RD, Johnson RL, Laufer E, Tabin C. 1993. Sonic hedgehog mediates the polarizing activity of the ZPA. Cell 75:1401–1416.

Roelink H, Augsburger A, Heemskerk J, Korzh V, Norlin S, Ruiz I Altaba A, Tanabe Y, Placzek M, Edlund T, Jessel TM. 1994. Floor plate and motor neuron induction by vhh-1, a vertebrate homolog of hedgehog expressed by the notochord. Cell 76:761–775.

Roth G, Wake DB. 1985. Trends in the functional morphology and sensorimotor control of feeding behavior in salamanders: an example of the role of internal dynamics in evolution. Acta Biol 34:175–192.

Roth G, Wake DB. 1989. Conservatism and innovation in the evolution of feeding in vertebrates. In: Wake DB, Roth G, editors. Complex organismal functions: integration and evolution in vertebrates. Chichester, UK: John Wiley & Sons. p 7–21.

Rubin L, Saunders JW. 1972. Ectodermal-mesodermal interactions in growth of limb buds in chick-embryo constancy and temporal limits of ectodermal induction. Dev Biol 28:94.

Sanz-Ezquerro JJ, Tickle C. 2003. Fgf signaling controls the number of phalanges and tip formation in developing digits. Curr Biol 13:1830–1836.

Saunders JW. 1948. The proximo-distal sequence of origin of the parts of the chick wing and the role of the ectoderm. J Exp Zool 108:363–403.

Saunders JW, Gasseling MT, Errick JE. 1976. Inductive activity and enduring cellular constitution of a supernumerary apical

ectodermal ridge grafted to limb bud of chick-embryo. Dev Biol 50:16–25.
Savage MP, Hart CE, Riley BB, Sasse J, Olwin BB, Fallon JF. 1993. Distribution of FGF-2 suggests it has a role in chick limb bud growth. Dev Dyn 198:159–170.
Schmalhausen II. 1907. Die Entwicklung des Skelettes der vordern Extremitat der anuren Amphibien. Anat Anz 31:177–187.
Schmalhausen II. 1910. Die Entwicklung des Extremitatenskelettes von *Salamandrelly kaiserlingii*. Anat Anz 37:431–446.
Schmalhausen II. 1915. Development of the extremities of the Amphibia and their significance to the question of the origins of the vertebrates. Moscow: University Press.
Shubin N, Alberch P. 1986. A morphogenetic approach to the origin and basic organization of the tetrapod limb. Evol Biol 20:319–387.
Shubin N, Wake DB. 1996. Phylogeny, variation, and morphological integration. Am Zool 36:51–60.
Sorensen EB, Mesner PW. 2005. IgH-2 cells: a reptilian model for apoptotic studies. Comp Biochem Phys B-Biochem Mol Biol 140:163–170.
Storm EE, Huynh TV, Copeland NG, Jenkins NA, Kingsley DM, Lee SJ. 1994. Limb alterations in brachypodism mice due to mutations in a new member of the TGF beta-superfamily. Nature 368:639–643.
Tickle C, Eichele G. 1994. Vertebrate limb development. Annu Rev Cell Biol 10:121–152.
Torok MA, Gardiner DM, Izpisua-Belmonte JC, Bryant SV. 1999. Sonic hedgehog (shh) expression in developing and regenerating axolotl limbs. J Exp Zool 284:197–206.
Vignali R, Nardi I. 1996. Unusual features of the urodele genome: do they have a role in evolution and development? Int J Dev Biol 40:637–643.
Vlaskalin T, Wong CJ, Tsilfidis C. 2004. Growth and apoptosis during larval forelimb development and adult forelimb regeneration in the newt (*Notopthalmus viridescens*). Dev Genes Evol 214:423–432.
Wake DB. 1982. Functional and evolutionary morphology. Perspect Biol Med 25:603–620.
Wake DB, Hanken J. 1996. Direct development in the lungless salamanders: what are the consequences for developmental biology, evolution and phylogenesis? Int J Dev Biol 40:859–869.
Wake DB, Larson A. 1987. Multidimensional analysis of an evolving lineage. Science 238:42–48.
Wake DB, Shubin N. 1998. Limb development in the Pacific giant salamanders, *Dicamptodon* (Amphibia, Caudata, Dicamptodontidae). Can J Zool 76:2058–2066.
Zakeri ZF, Ahuja HS. 1994. Apoptotic cell death in the limb and its relationship to pattern formation. Biochem Cell Biol 72:603–613.
Zeller R, Haramis AG, Zuniga A, McGuigan C, Dono R, Davidson G, Chabanis S, Gibson T. 1999. Formin defines a large family of morphoregulatory genes and functions in establishment of the polarizing region. Cell Tissue Res 296:85–93.